Physicochemical Properties of Polysaccharide Coatings Based on Grafted Multilayer Assemblies

Patrick G. Hartley,*,† Sally L. McArthur,‡ Keith M. McLean,†,‡ and Hans J. Griesser†,‡

CSIRO Molecular Science, Bag 10, Clayton South, Victoria 3169, Australia, and Co-operative Research Centre for Eye Research and Technology, University of New South Wales, Sydney, Australia

Received December 26, 2000. In Final Form: November 14, 2001

Carboxymethyldextrans of different charge densities have been attached to flat silicon wafer surfaces using plasma polymer interlayers in conjunction with two different chemical grafting strategies. The resultant coatings have been analyzed by XPS, to verify the surface coverage of the coatings and to estimate their dry thicknesses. Electrokinetic streaming potential measurement has been used to ascertain the electrostatic properties of the coatings, and atomic force microscope colloid probe force measurements have been used to provide insights into the extension of the polysaccharide chains from the interface in aqueous environments. The results demonstrate that polysaccharide layer thickness in solution is maximized when a secondary, amine-rich polyelectrolyte interlayer is introduced onto the plasma polymer surface prior to polysaccharide attachment. An increased carboxyl density in the polysaccharide has also been shown to give rise to thicker polymer layers in solution, with the electrokinetic properties of the resultant surfaces reflecting the charge density of the coupled polysaccharide. The data demonstrate that methods exist for tailoring the steric and electrostatic properties of interfaces based on the fine control of polysaccharide grafting.

Introduction

The adsorption of biological solutes has long been identified as a major determinant of the biological response to implanted biomaterials. Thrombogenesis, platelet activation, and immunogenic responses have all been shown to depend, at least in part, on the nature of the adsorbed layer which accumulates on a biomaterial surface in vivo.[1−3] Recent studies have also demonstrated how the selective adsorption of specific proteins to the surface can result in the mediation of cellular responses such as adhesion and migration.[4]

Polysaccharide coatings have been the focus of interest in biomaterials research by virtue of their ability to reduce this "fouling" of surfaces by biological species (particularly proteins) both in vitro and in vivo. A variety of polysaccharides have been explored for use as possible low-fouling surface modifications. These have included dextrans,[5−7] carboxymethylated dextrans,[8,9] and other carboxylated polysaccharides, such as hyaluronic acid and alginic acid.[10−12] In conjunction with these studies, a range of techniques have been employed in order to study and optimize the immobilization of polysaccharides at interfaces for protein adsorption studies. These have included direct adsorption,[10] adsorption of polysaccharide-based surfactants,[13] and various covalent coupling approaches, including the use of polyelectrolyte interlayers as graft enhancers.[6,7,14−16] The role of polysaccharide polymer graft density in particular has been explored by a number of groups, with the central conclusion that a well-pinned, dense polymer layer is required to prevent protein adsorption and cell adhesion.[5,6,17] Controversy exists as to the precise physicochemical properties possessed by polysaccharide and other hydrophilic polymer coatings which give rise to their "protein repellent" character.[18] Broadly speaking, protein repellency has been attributed either to the "physical" ability of a polymer layer to provide a steric/entropic barrier to adsorption[19,20] or to "chemical"

* To whom correspondence should be addressed. E-mail: Patrick.Hartley@molsci.csiro.au.

† CSIRO Molecular Science.

‡ University of New South Wales.

(1) Andrade, J. In *Surfaces and Interfacial Aspects of Biomedical Polymers. Volume 2*: *Protein Adsorption*; Andrade, J., Ed.; Plenum Press: New York, 1985; pp 1−80.

(2) Horbett, T.; Cooper, K.; Lew, K.; Ratner, B. *J. Biomater. Sci., Polym. Ed.* **1998**, *9* (10), 1071−1087.

(3) Pitt, W.; Park, K.; Cooper, S. L. *J. Colloid Interface Sci.* **1986**, *111*, 343−362.

(4) Horbett, T.; Ratner, B.; Schakenraad, J.; Schoen, F. In *Biomaterials Science*; Ratner, B. et al., Eds.; Academic Press: San Diego, 1996; p 133.

(5) Piehler, J.; Brecht, A.; Hehl, K.; Gauglitz, G. *Colloids Surf., B* **1999**, *13*, 325−336.

(6) Österberg, E.; Bergstrom, K.; Holmberg, K.; Schumann, T.; Riggs, J.; Burns, N.; Van Alstine, J.; Harris, J. *J. Biomed. Mater. Res.* **1995**, *29*, 741−747.

(7) Österberg, E.; Bergstrom, K.; Holmberg, K.; Riggs, J.; Van Alstine, J.; Schumann, T.; Burns, N.; Harris, J. *Colloids Surf., A* **1993**, *77*, 159−169.

(8) Löfås, S.; Johnsson, B. *J. Chem. Soc., Chem. Commun.* **1990**, 1526−1528.

(9) Dai, L.; Zientek, P.; St. John, H.; Pasic, P.; Chatelier, R. C.; Griesser, H. J. In *Surface Modification of Polymeric Biomaterials*; Ratner, B., Castner, D., Eds.; Plenum Press: New York, 1996; p 147.

(10) Morra, M.; Cassinelli, C.; Benedetti, L.; Callegaro, L. Patent WO 96/24392, 1996.

(11) Morra, M.; Cassinelli, C. *Langmuir* **1999**, *15*, 4658−4663.

(12) Morra, M.; Cassinelli, C. *J. Biomater. Sci., Polym. Ed.* **1999**, *10* (10), 1107−1124.

(13) Marchant, R. E.; Yuan, S.; Szakalas-Gratzl, G. *J. Biomater. Sci., Polym. Ed.* **1994**, *6* (6), 549−564.

(14) Brink, C.; Österberg, E.; Holmberg, K.; Tiberg, F. *Colloids Surf.* **1992**, *66*, 149−156.

(15) McArthur, S.; McLean, K.; Kingshott, P.; St. John, H.; Chatelier, R.; Griesser, H. *Colloids Surf., B* **2000**, *17* (1), 37−48.

(16) Frazier, R.; Matthijs, G.; Davies, M.; Roberts, C.; Schacht, E.; Tendler, S. *Biomaterials* **2000**, *21*, 957−966.

(17) Morra, M.; Cassinelli, C. *Surf. Interface Anal.* **1998**, *26* (10), 742−747.

(18) Morra, M. *J. Biomater. Sci., Polym. Ed.* **2000**, *11* (6), 547−569.

(19) Jeon, S. I.; Lee, J. H.; Andrade, J. D.; De Gennes, P. G. *J. Colloid Interface Sci.* **1991**, *142*, 149−158.

(20) Jeon, S. I.; Andrade, J. D. *J. Colloid Interface Sci.* **1991**, *142*, 159−166.

10.1021/la001801i CCC: $22.00
Published on Web 02/23/2002

interactions, particularly with water. In the latter case, the requirement for dehydration of a polysaccharide layer is thought to prohibit adsorption.[12]

With the exception of the cellulose surface (which has been extensively studied from the pulp and paper research viewpoint[21−26]), there has been surprisingly little attention paid to the direct measurement of the interactions experienced by proteins and other particles as they approach polysaccharide surfaces in aqueous environments.[22,27−30] Rather, emphasis has been placed on the use of indirect methods, most frequently spectroscopic, in deriving the molecular architectures of the coatings of interest.[11,31] These approaches yield important information regarding the internal composition of the coatings; however, the likelihood of structural rearrangement of such highly hydrated coatings during drying and/or evacuation cannot be ruled out.

In this study, we have attempted to address this problem by the application of colloid probe atomic force microscope (AFM) force measurement to the characterization of hydrated carboxymethyldextran (CMD) layers of varying charge density. We have used radio frequency glow discharge (rfgd) polymer films (also known as plasma polymers) to provide reproducible supports for the subsequent grafting of polysaccharide layers. These coatings provide an attractive substrate for use in biomaterials research as a result of their ability to introduce defined chemical functionalities at interfaces, within robust thin films which contour and adhere strongly to the surfaces of both organic and inorganic bulk materials.[32,33] The interfacial functionalities introduced in this way are then readily accessible for subsequent grafting reactions via an array of coupling strategies.[34,35]

In addition to AFM colloid probe force measurement, we have also employed streaming potential determination to estimate the contribution of electrostatic interactions to the forces experienced by a particle approaching the charged polysaccharide surfaces.

Polysaccharide pinning densities have been varied by the application of additional polyelectrolyte interlayers. Additional surface chemical characterization has also been achieved using X-ray photoelectron spectroscopy (XPS).

In parallel with these studies and reported elsewhere, we have investigated the protein adsorption characteristics of the surfaces with a variety of techniques[15,36] and finally studied the cellular response to them.[37] In this way, we have attempted to interpret the dominant physicochemical factors which allow polysaccharide graft layers to act as protein repellent or protein selective coatings and to ascertain how such factors influence cell attachment.

Experimental Section

Materials. Silicon wafers (1 cm^2 square) with a 17 nm oxide layer were cut from 150 mm diameter wafer disks obtained from Quality Semiconductor Australia, Homebush, NSW. Prior to experiment, the squares were ultrasonicated in pure AR ethanol and rapidly blown dry in a stream of filtered nitrogen gas. XPS analysis of wafer samples prepared in this way indicated minimal levels of carbonaceous contamination (∼6−9 atomic % carbon).

Colloidal silica spheres of ∼5 μm diameter were obtained from Allied Signal, Illinois. The electrokinetic and force measurement characteristics of these particles have been described in detail earlier.[38]

n-Heptylamine (99%) and acetaldehyde (>99%) used in plasma polymerization were obtained from Sigma-Aldrich, Castle Hill, NSW.

All glassware and AFM fluid-contact components used in this study were cleaned in an ultrasonic bath for 2 h in a solution of 5% RBS surfactant (Pierce Chemicals)/10% AR grade ethanol in Milli-Q water, followed by rinsing in copious quantities of Milli-Q water.

XPS analysis of test samples cleaned in this way indicated minimal carbonaceous surface contamination from the cleaning protocol (∼6−9 atomic % carbon).

Phosphate-buffered saline at pH 7.4 (PBS) used in these experiments was prepared in Milli-Q water using AR grade NaCl (0.137 M), Na_2HPO_4 (0.01 M), NaH_2PO_4 (0.002 M), and KCl (0.003 M). Dilutions were made from this "1× PBS" solution in Milli-Q water.

Plasma Polymerization. Plasma polymerization of *n*-heptylamine and acetaldehyde was carried out in a custom-built reactor as described elsewhere.[39] Briefly, the cylindrical reactor chamber is defined by a height of 35 cm and a diameter of 17 cm. Clean silicon wafer samples were placed on the lower circular electrode (diameter, 9.5 cm), with the upper electrode U-shaped. The distance between the electrodes was 12.5 cm. The parameters chosen for the plasma deposition of *n*-heptylamine were a frequency of 200 kHz, a power of 20 W, and an initial monomer pressure of 16.67 Pa. The treatment time was 20 s. This results in a plasma polymer film thickness of 40 nm. For acetaldehyde, the conditions were 125 kHz, 10 W, and 40 Pa for 1 min, yielding films of 30 nm in thickness. Thicknesses were obtained by AFM measurement of step heights of plasma polymer boundaries on samples prepared under identical conditions on silicon wafers as described in ref 40.

Polymer Grafting Reactions. Poly(ethyleneimine) (PEI, 70 000 MW, Sigma-Aldrich, Castle Hill, NSW) was attached directly to acetaldehyde plasma polymer surfaces (Aapp) using reductive amination.[41] A 3 mg/mL solution of PEI was prepared in water, and once the solute had dissolved, the pH was adjusted to 7.4 with 1 M HCl. Freshly prepared plasma surfaces were then immersed in the PEI solution. The surfaces were incubated in the polymer for 30 min prior to addition of 3 mg/mL of sodium cyanoborohydride ($NaCNBH_3$, Sigma-Aldrich, Castle Hill, NSW). The reductive amination reaction was then allowed to proceed overnight.

Dextran (70 000 MW, Sigma-Aldrich, Castle Hill, NSW) was carboxymethylated using a published procedure.[15] In brief, 10 g of dextran was dissolved in 50 mL of 2 M NaOH containing levels of bromoacetic acid between 0.25 and 1.0 M. The solution

(21) Claesson, P. M.; Ninham, B. W. *Langmuir* **1992**, *8*, 1406−1412.
(22) Claesson, P. In *Biopolymers at Interfaces*; Malmsten, M., Ed.; Marcel Dekker: New York, 1998; pp 281−320.
(23) Carambassis, A.; Rutland, M. W. *Langmuir* **1999**, *15*, 5584−5590.
(24) Holmberg, M.; Wigren, R.; Erlandsson, R.; Claesson, P. M. *Colloids Surf., A* **1997**, *129−130*, 175−183.
(25) Poptoshev, E.; Rutland, M. W.; Claesson, P. M. *Langmuir* **2000**, *16*, 1987−1992.
(26) Zauscher, S.; Klingenberg, D. J. *J. Colloid Interface Sci.* **2000**, *229*, 497−510.
(27) Rau, D.; Parsegian, V. *Science* **1990**, *249*, 1278.
(28) Malmsten, M.; Claesson, P. *Langmuir* **1991**, *7*, 988−994.
(29) Wigren, R.; Billsten, P.; Erlandsson, R.; Lofas, S.; Lundstrom, I. *J. Colloid Interface Sci.* **1995**, *174*, 521−523.
(30) Morra, M.; Cassinelli, C. *Colloids Surf., B* **2000**, *18*, 249−259.
(31) Harder, P.; Grunze, M.; Dahint, R.; Whitesides, G. M.; Laibinis, P. E. *J. Phys. Chem. B* **1998**, *102*, 426−436.
(32) Ratner, B.; Chilkoti, A.; Lopez, G. In *Plasma Deposition, Treatment, and Etching of Polymers*; d'Agostino, R., Ed.; Academic Press: San Diego, 1990; pp 463−516.
(33) Griesser, H. J. *Mater. Forum* **1990**, *14*, 192−202.
(34) Griesser, H.; McLean, K.; Beumer, G.; Gong, X.; Kingshott, P.; Johnson, G.; Steele, J. *Mater. Res. Soc. Symp. Proc.* **1999**, *544*, 9.
(35) Dai, L.; St. John, H.; Bi, J.; Zientek, P.; Chatelier, R.; Griesser, H. *Surf. Interface Anal.* **2000**, *29*, 46−55.
(36) McArthur, S. L.; McLean, K.; Hartley, P. G.; Griesser, H. J. Manuscript in preparation.
(37) McLean, K.; McArthur, S. L.; Johnson, G.; Griesser, H. J. Manuscript in preparation.
(38) Hartley, P. G.; Larson, I.; Scales, P. J. *Langmuir* **1997**, *13* (8), 2207−2214.
(39) Griesser, H. J. *Vacuum* **1989**, *39*, 485.
(40) Hartley, P. G.; Vaithianathan, T.; Thissen, H.; Griesser, H. J. *Plasmas Polym.* **2000**, *5* (1), 47−60.
(41) Hermanson, G. T. *Bioconjugate techniques*; Academic Press: San Diego, 1996.

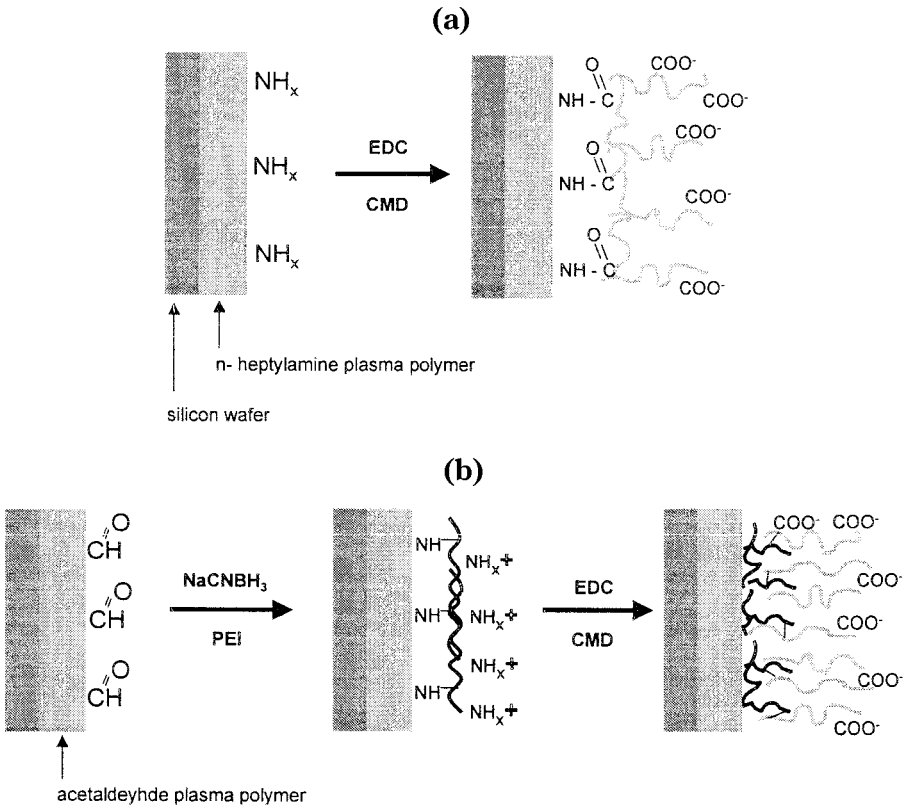

Figure 1. Schematic of the plasma polymer/grafting reactions used in this study. (a) Direct grafting of CMD layers on heptylamine plasma polymers via water-soluble carbodiimide (EDC) chemistry. (b) Grafting of CMDs on acetaldehyde plasma polymers via PEI interlayers. The PEI is first grafted to the surface via reductive amination. Subsequent attachment of CMDs is achieved using water-soluble carbodiimide (EDC) chemistry.

was stirred overnight and then dialyzed (8000 MW cutoff) against Milli-Q water for 24 h, then 0.1 M HCl for 24 h, and finally for 24 h against Milli-Q water. The product was then lyophilized and stored at 4 °C until required.

Varying the level of bromoacetic acid enabled the ratio of carboxyl groups per anhydroglucopyranoside (Glc) ring to be varied between 1:2 to 1:30. Back-titration and NMR were used to determine the extent of carboxylation.

CMDs were grafted onto either *n*-heptylamine (Happ) or Aapp/PEI surfaces using water-soluble carbodiimide chemistry.[41] Solutions (2 mg/mL) of the CMDs were prepared. Once dissolved, 19.8 mg/mL of *N*-hydroxysuccinimide (NHS, Sigma-Aldrich, Castle Hill, NSW) and 12 mg/mL of (1-ethyl-3-(3-dimethylaminopropyl) carbodiimide (EDC, Sigma-Aldrich, Castle Hill, NSW), respectively, were added, and the substrate surfaces of interest were immersed in the resultant solution. The reaction was allowed to proceed overnight at room temperature. The surfaces were rinsed in a copious volume of Milli-Q water prior to analysis. The chemical construction of the two types of polysaccharide-bearing surfaces is summarized in Figure 1.

XPS. XPS analysis was performed using an AXIS HSi spectrometer (Kratos Analytical Ltd, U.K.) equipped with a monochromatic Al Kα source at a power of 300 W. The pressure in the main vacuum chamber during analysis was typically 5×10^{-8} mbar. Elements present were identified from survey spectra. For further analysis and quantification, spectra were recorded from individual peaks at 80 eV pass energy. High-resolution spectra were also collected at 40 eV.

Atomic concentrations of each element were calculated by determining the relevant integral peak intensities and applying the sensitivity factors supplied by the instrument manufacturer. A linear background was used in all cases. The random error associated with elemental quantification has been determined, for this instrument, to be 1−2% of the absolute values for atomic percentages in the range encountered in this study (>5 atom %).[42] The systematic error is much more difficult to determine and is generally assumed to be of the order of 5−10%.[43] It is the random error that is more relevant when comparing samples of similar composition.

Table 1. Elemental Compositions of Polymer Surfaces on Silicon Wafers Derived from High-Resolution XPS Spectra

	atomic concentration %				atomic ratio	
surface	C1s	O1s	N1s	Si2p	N/C	O/C
HApp	86.2	6.7	7.0	0.0	0.08	0.08
+ CMD 1:2	72.5	21.7	5.8	0.0	0.08	0.30
+ CMD 1:30	75.2	18.1	6.5	0.2	0.09	0.24
AApp	84.7	14.6	0.2	0.5	<0.01	0.17
+ PEI	80.3	14.5	5.1	0.1	0.06	0.18
+ PEI + CMD 1:2	66.3	29.2	4.0	0.5	0.06	0.44
+ PEI + CMD 1:30	71.2	22.9	5.2	0.7	0.07	0.32
pure PEI	72.5	1.0	26.6	0.0	0.37	0.01
pure CMD 1:2	55.4	44.6	0.0	0.0	0.0	0.81
pure CMD 1:30	53.9	46.1	0.0	0.0	0.0	0.86

Depending on the dominant C1s component peak in each sample, reference binding energies of either 285.0 eV (CH_x) or 286.7 eV (C−O) were used to correct for offsets due to incomplete charge neutralization of specimens under irradiation (typically ~3.5 eV in this case).[44] A value of ~3 nm for the electron attenuation length of a C1s photoelectron in a polymeric matrix was assumed.[43] This translates into an approximate value for the XPS analysis depth (from which 95% of the detected signal originates) of 10 nm when recording XPS data at an emission angle normal to the surface.

Elemental compositions for pure polymer/polysaccharide shown in Table 1 were derived from spectra recorded from thick polymer samples prepared by drying concentrated solutions on silicon wafer surfaces. Quantification was only performed on

(42) Gengenbach, T. R. Personal communication, 2000.

(43) Gengenbach, T. R.; Vasic, Z. R.; Chatelier, R. C.; Griesser, H. J. *J. Polym. Sci., Part A: Polym. Chem.* **1994**, *32*, 1399−1414.

(44) Beamson, G.; Briggs, D. *High-Resolution XPS of Organic Polymers*; John Wiley & Sons: Chichester, 1992.

these samples when no silicon substrate signals were detectable from the XPS survey spectra.

Electrokinetic Streaming Potential Measurements. The streaming potential apparatus was based on the design of Van Wagenen,[45] and its operation is described in detail elsewhere.[46]

The apparatus, which was constructed almost exclusively of fluoropolymer-based materials (Teflon/Delrin) was cleaned prior to use by sequential circulation of 0.1 M solutions of NaOH and HNO_3, with copious rinsing using Milli-Q water between each circulation.

The streaming potential of coated glass slides (ΔV) was related to ζ potential using the Smoluchowski equation:[47]

$$\zeta = \frac{\eta\lambda}{\epsilon_0\epsilon_r}\frac{\Delta V}{\Delta P} \quad (1)$$

where ΔP represents the pressure drop across the capillary formed between the surfaces of interest, λ is the conductivity of the capillary, η is the viscosity of water, and $\epsilon_0\epsilon_r$ is the dielectric constant of the aqueous medium. Dilute HCl or NaOH was used to adjust the pH during titrations. The conductivity of the capillary, λ, was assumed to equal the specific conductivity of the bulk electrolyte solution, which has been shown previously to be a reasonable assumption for the cell geometry and 1 mM electrolyte concentration employed in these experiments.[46] This electrolyte concentration was also employed in order to minimize the amplification of errors due to higher conductivity electrolyte solutions increasing the prefactor in eq 1.

The Smoluchowski approach is valid in the interpretation of streaming potential data for flat, nonstructured surfaces, in electrolyte conditions where surface conduction effects are minimal.[45] Analysis of plasma polymer surfaces identical to those employed herein suggests that these conditions are met for such interfaces, and thus the Smoluchowski analysis is appropriate.[40]

We note, however, that the introduction of structure at the interface by the grafting of charged polymer layers atop the plasma polymer surfaces complicates data interpretation considerably. In such cases, the Smoluchowski conditions of infinite viscosity and fixed charges at the shear plane, as well as a less than complete understanding of surface conduction and hydrodynamics in these systems, mean that use of the Smoluchowski equation is somewhat inappropriate. However, correction of the data to incorporate these considerations is complex and was thought to impact little on the conclusions of this work. The reader is, however, advised to treat the ζ potential values calculated for such surfaces as semiquantitative at best.[48]

AFM Colloid Probe Force Measurements. A Digital Instruments (Santa Barbara, CA) Nanoscope multimode AFM was used in the force measuring experiments. Measurements were performed using the standard fluid cell/O-ring/tubing equipment supplied by Digital Instruments. Gold-coated silicon nitride cantilevers used in the AFM experiments were obtained in wafer form from Digital Instruments. Several cantilevers were selected from different regions of the wafer, and their spring constants were determined by the method of Cleveland et al.[49] Cantilevers used in this study had spring constants of 0.08 or 0.16 N/m and were modified for force measurements by attaching $\sim$5 μm diameter silica spheres at the apex of the cantilevers using an extremely small quantity ($\sim 1 \times 10^{-15}$ L) of Epikote 1004 adhesive.[50] The radius of the spheres used in each experiment was measured using a light microscope to an accuracy of $\pm$0.14 μm. AFM substrates bearing mounted colloid probes were soaked for at least 1 h in 6% H_2O_2, rinsed in Milli-Q water, and then dried in a filtered nitrogen stream prior to force measurement. In some cases, a 30 min UV ozone treatment was instead employed. XPS analysis of silicon wafer surfaces cleaned using both approaches revealed similar low levels of carbon-containing species on the surfaces following immersion in Milli-Q water.

Assembly of the AFM prior to experimentation was performed in a laminar flow clean air cabinet.

Analysis of AFM Colloid Probe Force Measurements. Raw AFM tip deflection versus travel data were converted into force versus separation data using the established method.[50] A major source of error in this procedure arises from the nomination of a zero separation position. This is generally assumed to coincide with the position at which the deflection of the AFM tip is linear with respect to the displacement of the sample surface, termed the "constant compliance" regime. While use of this relationship is reasonable for interactions between hard, flat surfaces, it may not in fact represent the position at which a compressible polymer layer is fully excluded or "squeezed out" from the gap between the supporting surfaces. Instead, the constant compliance behavior may occur at some finite compression of the polymer layer.

In this case, therefore, the separation calculated from the raw data is relative to maximum layer compression rather than a true zero separation. For this reason, force−distance data are presented in this paper with "relative separation" as the *x*-axis label.

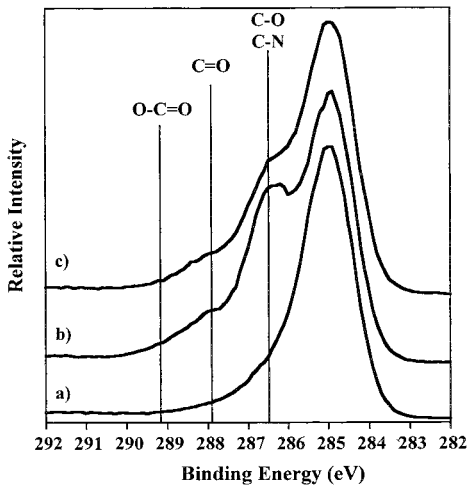

Figure 2. (a) High-resolution XPS C1s spectrum of a fresh Happ surface. (b) High-resolution XPS C1s spectrum of a Happ surface bearing grafted CMD 1:2. (c) High-resolution XPS C1s spectrum of a Happ surface bearing grafted CMD 1:30. The spectra have been displaced relative to each other in the *y*-direction to allow comparison of peak positions.

Results and Discussion

XPS Analysis of *n*-Heptylamine Plasma Polymer (Happ) Based Coatings. XPS analysis of a freshly deposited *n*-heptylamine plasma polymer on silicon wafers (Figure 2a and Table 1) indicated a polymer rich in hydrocarbon- and nitrogen-containing species, as has been observed previously on different substrates.[51] The broad C1s peak is associated with the variety of chemical structures formed during polymer deposition from the gas plasma. As a result, it is difficult to clearly resolve the C−N containing species from those containing C−O which may result from the spontaneous quenching of carbon radicals within the film on exposure to air. Previous studies using derivatization have, however, indicated that these coatings have an amine density of 0.5−2.0 amines/nm^2.[52]

(45) Van Wagenen, R. A.; Andrade, J. D. *J. Colloid Interface Sci.* **1980**, *76* (2), 305−314.
(46) Scales, P. J.; Grieser, F.; Healy, T. W.; White, L. R.; Chan, D. Y. *Langmuir* **1992**, *8*, 965−974.
(47) Hunter, R. J. *The Zeta Potential in Colloid Science*; Academic Press: London, 1981.
(48) Ohshima, H.; Kondo, T. *J. Colloid Interface Sci.* **1990**, *135* (2), 443−448.
(49) Cleveland, J. P.; Manne, S.; Bocek, D.; Hansma, P. K. *Rev. Sci. Instrum.* **1993**, *64* (2), 403−405.
(50) Ducker, W. A.; Senden, T. J.; Pashley, R. M. *Nature* **1991**, *353*, 239−241.
(51) Gengenbach, T. R.; Chatelier, R. C.; Griesser, H. J. *Surf. Interface Anal.* **1996**, *24*, 271−281.
(52) Griesser, H. J.; Chatelier, R. C. *J. Appl. Polym. Sci.: Appl. Polym. Symp.* **1990**, *46*, 361−384.

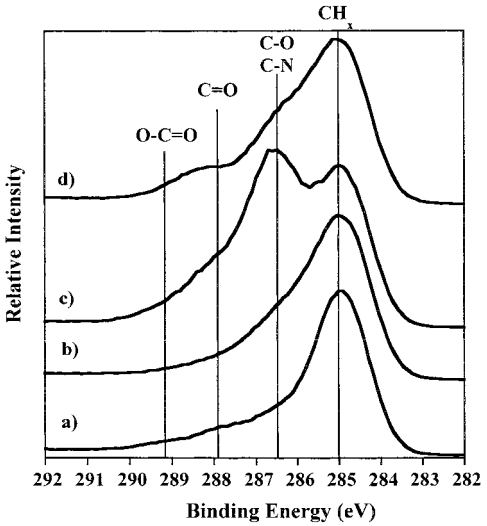

Figure 3. (a) High-resolution XPS C1s spectrum of a fresh Aapp surface. (b) High-resolution XPS C1s spectrum of Aapp bearing grafted PEI. (c) High-resolution XPS C1s spectrum of Aapp−PEI−CMD 1:2. (d) High-resolution XPS C1s spectrum of Aapp−PEI−CMD 1:30. The spectra have been displaced relative to each other in the *y*-direction to allow comparison of peak positions.

The reduction in silicon atomic concentration from ∼37% for an uncoated oxidized silicon wafer (data not shown) to zero when plasma polymer coated also indicates a >10 nm thick, pinhole-free plasma polymer layer. This has been confirmed by AFM imaging, which shows films prepared identically to be 35−40 nm in thickness and of smooth topology.[40]

Table 1 and Figure 2b,c show the analysis of XPS C1s spectra of *n*-heptylamine-modified silicon wafer samples following EDC/NHS-mediated grafting of CMD 1:2 and CMD 1:30. Table 1 in particular shows the significant increases in the oxygen content relative to the *n*-heptylamine plasma polymer surface, confirming the attachment of polysaccharide to the surface.

To compare the high-resolution C1s peak positions, the spectra were shifted to ensure that the leading edges of the fitted CH_x component were coincident. All spectral intensities were then normalized to a maximal intensity corresponding to the full height of the fitted CH_x (285 eV) component peak. As shown in Figure 2, the increase in oxygen content in the films is readily explained by an accumulation of oxygen-containing carbon species associated with the polysaccharide. Of particular note is the increase in the peak at 289 eV relative to the plasma polymer, indicative of carboxyl incorporation at the surface.

Simple overlayer calculations based on the attenuation of the N1s photoelectron signals from the plasma polymer by the grafted layers (see Table 1) suggest layer thicknesses of 0.6 and 0.2 nm for the CMD 1:2 and CMD 1:30 layers, respectively, in the dry/evacuated state.[53]

XPS Analysis of Aapp-Based Coatings. Figure 3a shows an XPS analysis of a freshly deposited acetaldehyde plasma polymer. The disappearance of the substrate silicon signal again indicates a >10 nm thick pinhole-free coating. AFM step height analysis of these coatings[40] has shown them to be ∼30 nm in thickness. The spectrum shows a polymer rich in hydrocarbon- and oxygen-containing species. Once again, the broad C1s spectrum provides evidence of secondary peak shifts, complicating peak assignation. However, there is strong evidence for the presence of C−O, C═O, and O−C═O functional groups in the coating. In this case, these oxygen-containing species within the film may be due solely to reactions within the plasma during film deposition or additionally the result of postplasma oxidation as described above. Studies currently under way in our laboratory show that such films oxidize rapidly within the first 48 h after deposition.

The XPS C1s spectrum of PEI grafted onto the rfgd-deposited acetaldehyde is shown in Figure 3b. The increase in nitrogen content (but not oxygen) shown in Table 1 suggests that the increase in height of the C1s shoulder at 286.5 eV is attributable to the presence of C−N species of the PEI.

The ratio of atomic concentrations of nitrogen to carbon (N/C) for this coating (0.06) was considerably smaller than the 0.5 expected for a pure PEI coating. This demonstrates that the PEI coating is either extremely thin or that its coverage of the surface is not complete. Gross heterogeneity in the coatings is ruled out by the reproducibility of XPS measurements across the surface, while AFM force data (which are discussed later) also appear to rule out microscale heterogeneities. Once again, an overlayer calculation based on the concentration of nitrogen in the grafted polymer relative to the nitrogen content of a "pure" PEI thick film (see Table 1) gives a layer thickness of 0.7 nm in the dry/evacuated state.[53]

Figure 3c,d and Table 1 show the effect on the XPS spectra of the attachment of CMD 1:2 and CMD 1:30 to the acetaldehyde−PEI surface.

The introduction of C−O (286.5 eV), C═O (287.9 eV), and O−C═O (289.2 eV) observed in the high-resolution C1s spectra indicated the successful grafting of both CMDs onto the PEI interlayer, with the higher carboxyl density CMD 1:2 producing the largest effect, suggesting a higher grafting efficiency. The lack of significant attenuation of the N1s signal from the PEI layer following CMD 1:30 grafting may also suggest that in this case, PEI is present at the outer surface of the coating, possibly as a result of intercalation within the polysaccharide layer. Another possibility is that this represents an artifact due to structural rearrangement of the coating during dehydration/evacuation prior to XPS analysis. This possibility precludes the calculation of CMD layer thicknesses from the XPS data using overlayer models. However, the significant contribution to the C1s spectrum from the C−C peak at 285 eV presumably originates largely from the underlying plasma polymer suggesting that the overlayer thickness does not exceed the XPS sampling depth of ∼10 nm. AFM thickness measurements using a masking method also show that the dry thickness of the layers is in the range of 2−12 nm.[40,54]

Streaming Potential Analysis of Happ-Based Coatings. Figure 4a shows the results of streaming potential measurements performed on glass surfaces bearing heptylamine plasma polymer and subsequently grafted polysaccharide coatings in 0.001 M sodium chloride at different pHs. The measured streaming potentials have been converted to ζ potential values using the Smoluchowski equation, as detailed in the Experimental Section.

The isoelectric point of the unmodified heptylamine plasma polymer surface is found to be ∼pH 5, with an approach to a plateau value of −70 mV at pH values greater than 8. Assuming purely anionic charge site dissociation in the high pH regime and that the ζ potential reasonably approximates the diffuse layer potential in

(53) *Practical Surface Analysis*; Briggs, D., Seah, M. P., Eds.; John Wiley and Sons: Chichester, 1995; Vol. 1.

(54) McArthur, S. L. Ph.D. Thesis, University of New South Wales, Sydney, Australia, 2000.

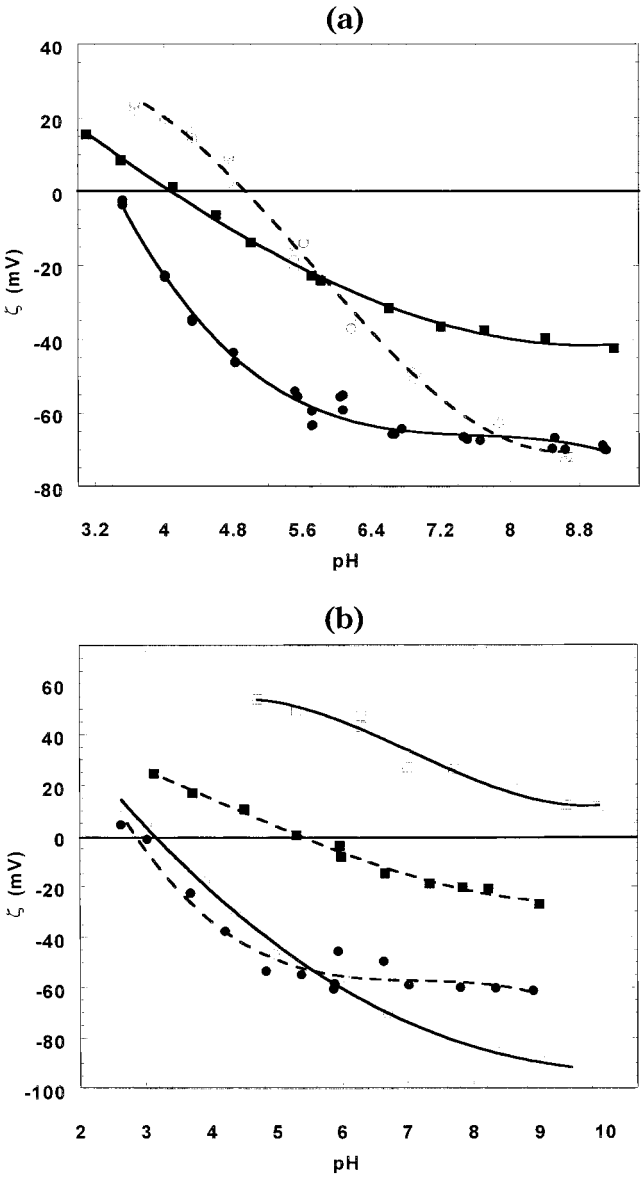

Figure 4. Streaming potential measurements of polymer coatings recorded in 1 mM NaCl: (a) ○, Happ; ●, Happ + CMD 1:2; ■, Happ + CMD 1:30; (b) ○, Aapp; □, Aapp + PEI; ●, Aapp + PEI + CMD 1:2; ■, Aapp + PEI + CMD 1:30.

these conditions, the Guoy−Chapman equation may be used to derive a surface charge density of 0.8 μC/cm^2.[47]

Assuming that at pH 4 the surface charge is composed purely of cationic surface groups, the ζ potential value of +25 mV suggests a surface charge density of 0.22 μC/cm^2 using the same calculation. These values correspond to 0.05 and 0.014 charges/nm^2, respectively.

We note that the latter value is considerably lower than measurements of amine surface densities on heptylamine plasma polymers derived from XPS labeling experiments (0.5−2 amines/nm^2).[52] Such discrepancies have been frequently observed, particularly in measurements of titratable surface groups, which generally greatly exceed charge densities calculated using the above approach.[47,55] We further note that carboxyl functionalities are not apparent at the characteristic 289 eV position in the high-resolution C1s XPS spectrum (Figure 2a). Thus, the origin of the anionic groups on the plasma polymer surface is unclear.

We note, however, that this plasma polymer surface is somewhat hydrophobic, with an advancing water contact angle of 79° at the pH of these experiments.[56] The literature shows considerable precedent for the acquisition of negative charges by hydrophobic surfaces of various types, frequently thought to be due to specific adsorption of anions (e.g., bicarbonate) from solution.[57,58]

Another possibility is that acidic groups are in fact present on the plasma polymer top surface, but in such low levels that they are below the XPS analysis sensitivity. As described above, the Guoy−Chapman equation can be used to produce an estimate of the charge density of the surface under investigation. Assuming a surface potential for heptylamine plasma polymer of −60 mV at pH 7.4 in 10^{-3} M 1:1 electrolyte (see Figure 4a), we obtain ∼29 nm^2 per charged group. It seems quite plausible that such a low surface concentration could be below XPS sensitivity.

The reader is referred to the Experimental Section with regard to difficulties in the interpretation of streaming potential data on the polysaccharide-grafted surfaces. However, qualitatively the effect of attachment of the low carboxyl density carboxymethyldextran (CMD 1:30) is to reduce the isoelectric point of the surface (to ∼pH 4.1) and also to reduce the pH at which the ζ potential plateaus (to pH ∼ 7). In addition, the magnitude of the high pH potential plateau is reduced to ca. −35 mV.

The downward shift in the isoelectric point of the CMD-modified surface relative to the bare plasma polymer has one of two explanations:

(1) The acidic groups on the plasma polymer have not been fully "masked" by the presence of the polysaccharide, with the "net" pK_a of the surface shifted downward due to consumption of surface amines in the EDC/NHS coupling reaction.

(2) New acidic groups associated with the carboxymethyldextran (and with a different pK_a to the plasma polymer acidic moieties) have been incorporated on the surface.

It is not possible to unequivocally dismiss either option based on these measurements. However, the latter explanation is supported by the XPS data in Figure 2, since carboxyl species are detectable on the surface only after polysaccharide grafting.

The lowering of the plateau potential of the CMD 1:30 grafted surface at high pH relative to the underlying heptylamine plasma polymer surface does, however, demonstrate that the anionic surface charge density of the CMD 1:30 modified surface is lower than that of the bare plasma polymer. This is perhaps not surprising considering the low density of charged groups of this polysaccharide.

The effect of attachment of the high carboxyl density polysaccharide CMD 1:2 onto the heptylamine plasma polymer surface is to further reduce the isoelectric point of the surface to ∼pH 3.5. This suggests a further change in the pK_a of the charged groups as described above and is consistent with the significantly higher carboxyl content found in the XPS C1s spectra at 289 eV (see Figure 2b).

The plateau potential found at high pH for this surface is also attained at ∼pH 6.4, suggesting that the acidic groups responsible for the charging process on both the CMD 1:30 and CMD 1:2 surface have similar chemistries.

(55) Van Wagenen, R. A.; Coleman, D. L.; King, R. N.; Triolo, P.; Brostrom, L.; Smith, L. M.; Gregonis, D. E.; Andrade, J. D. *J. Colloid Interface Sci.* **1981**, *84* (1), 155−162.

(56) Chatelier, R. C.; Drummond, C. J.; Chan, D. Y. C.; Vasic, Z. R.; Gengenbach, T. R.; Griesser, H. J. *Langmuir* **1995**, *11* (10), 4122−4128.

(57) Meagher, L.; Pashley, R. M. *Langmuir* **1995**, *11*, 4019−4024.

(58) Hartley, P. G.; Grieser, F.; Mulvaney, P.; Stevens, G. W. *Langmuir* **1999**, *15*, 7282−7289.

The behavior is also consistent with carboxyl groups dominating the surface charge, as would be expected for these polysaccharides. Finally, the greater magnitude of the plateau potential at high pH (ca. −70 mV) is indicative of a considerably higher carboxyl density on the CMD 1:2 surface, again consistent with the molecular architecture of this highly carboxylated polysaccharide.

Streaming Potential Analysis of Acetaldehyde Plasma Polymer Based Coatings. As is shown in Figure 4b, the unmodified acetaldehyde plasma polymer surface is found to be considerably more acidic than the heptylamine plasma polymer, with an isoelectric point at ∼pH 3.2. This is consistent with the carboxyl functionality detected in the XPS data at 289 eV in Figure 3a. A dramatic charge reversal occurs on the surface following the grafting of the cationic polyelectrolyte PEI. This surface is positive at all pH values, indicating that a high degree of basic amine groups have been incorporated at the interface, and would appear to rule out sparseness of the layer, as mentioned earlier in the discussion of XPS data. This is also consistent with the high density of amine groups on the PEI chains relative to the aldehyde groups on the plasma polymer surface, which allows a significant PEI amine fraction to remain unconsumed during and after the grafting reaction.

Subsequent attachment of the low charge density polysaccharide CMD 1:30 generates a surface of relatively low ζ potential at all pH values, with an isoelectric point at pH 5.4. This indicates that the CMD 1:30 attachment has effectively neutralized the PEI surface either by complete consumption of ionizable groups during the amine−carboxyl reaction in the grafting reaction or by additional charge complexation interactions between carboxyl and amine functionalities on the two polymers.

While the magnitude and signs of the ζ potential measurements are different, qualitatively similar trends in the pH versus ζ potential relationship exist between the PEI−Aapp and CMD 1:30−PEI−Aapp surfaces. This, coupled with the observation that the detection of an isoelectric point for this surface implies the presence of protonatable surface groups, may further indicate a contribution to the electrokinetic behavior from the PEI within the coating. The implication here is that the PEI is distributed throughout the graft layer, forming an "amphoteric" coating, and not purely as a "boundary layer" between the plasma polymer and polysaccharide coatings. This hypothesis is supported by the XPS data for this surface (see Table 1) which demonstrate minimal attenuation of the N1s signal from the polyelectrolyte interlayer following addition of the polysaccharide layers.

The electrokinetic behavior of the CMD 1:2 grafted PEI−Aapp surface is very similar to that of the heptylamine−CMD 1:2 surface. The fact that the support surfaces used to prepare these coatings have very different electrokinetic properties suggests that in both cases the electrokinetic behavior of the subsequent grafted surfaces is dominated by the polysaccharide charge density.

AFM Colloid Probe Force Measurements on Surfaces prior to Polysaccharide Attachment. Figure 5a,b shows typical results of AFM surface force measurements performed between a silica colloid probe and the two plasma polymer support surfaces used for attachment of polysaccharides, at two different electrolyte concentrations.

At the lower electrolyte concentration (1:100 PBS, effective [electrolyte] = 0.00152 M), the force versus separation relationships between the silica colloid probe and the untreated plasma polymer surfaces were characterized by exponentially increasing repulsions as the surfaces approached, which gave way to a hard wall repulsion, nominated as the zero separation position. In some cases, this transition was marked by a slight discontinuity in the data, indicating a small "jump" together of the surfaces. The measured decay lengths of the exponential components of the interactions are shown in Table 2 and were in excellent agreement with the theoretically predicted Debye length ($1/\kappa$) for the mixed electrolyte system, which was calculated assuming the correct proportions of 1:1 and 3:1 electrolyte for the phosphate-buffered saline system.[47] While the use of this electrolyte system adds complications to data interpretation, we were keen to simulate as accurately as possible the conditions used in protein adsorption and cell attachment experiments the results of which will appear elsewhere.[36,37]

Table 2. Comparison of Force Law Decay Lengths Derived from Surface Force Measurements in Different PBS Dilutions with Theoretical Decay Lengths

interaction	[PBS] dilution	Debye length $1/\kappa$ (nm)	measured decay length (nm)
silica−Happ	1:100	6.6	7.5
silica− Aapp	1:100	6.6	6.8
silica−PEI/Aapp	1:100	6.6	6.8
silica−Happ−CMD 1:2	1:100	6.6	9.94
	1:10	2.1	6.6
	1:1	0.7	3.9
Si−Happ−CMD 1:30	1:100	6.6	6.8
	1:10	2.1	2.43
	1:1	0.7	1.4
Si−Aapp−PEI−CMD 1:2	1:100	6.6	16
	1:10	2.1	10.7
	1:1	0.7	5.6
Si−Aapp−PEI−CMD 1:30	1:100	6.6	9.1
	1:10	2.1	12
	1:1	0.7	7.5

The fact that the decay lengths of the measured interactions are in good agreement with the calculated values is a strong indicator of a purely electrostatic interaction mechanism. Further support for this assertion is provided by surface force measurements at the higher electrolyte concentration (pure PBS, effective 1:1 [electrolyte] = 0.152 M) which showed no effective interaction prior to the zero separation hard wall repulsion. This removal of exponential repulsion is to be expected if the interaction is electrostatic in origin and is due to compression of the electrical double layers between the surfaces. In this case, the theoretical Debye length of the electrolyte system is 0.66 nm, and hence the interactions decay much more rapidly than in the dilute electrolyte case. Under these conditions, one might expect to observe an attractive force between the silica colloid probe and the plasma polymer surface due to van der Waals forces acting between them. The lack of such an interaction in the silica−aqueous−heptylamine interaction (Figure 5a) may indicate a weak van der Waals force (i.e., low Hamaker constant).

Calculation of the heptylamine−aqueous−heptylamine Hamaker constant from optical properties using the Lifshitz approach yields a zero separation (nonretarded) value of 1.16×10^{-20} J.[59] Using a simple combining relation with the value for silica−aqueous−silica of 0.85×10^{-20} J,[38,60] we obtain an approximate value of 0.99×10^{-20} J for the silica−aqueous−heptylamine interaction, which approaches the low values found for silica surfaces

(59) Meagher, L. Personal communication, 2001.
(60) Israelachvili, J. N. *Intermolecular and Surface Forces*, 2nd ed.; Academic Press: London, 1992.

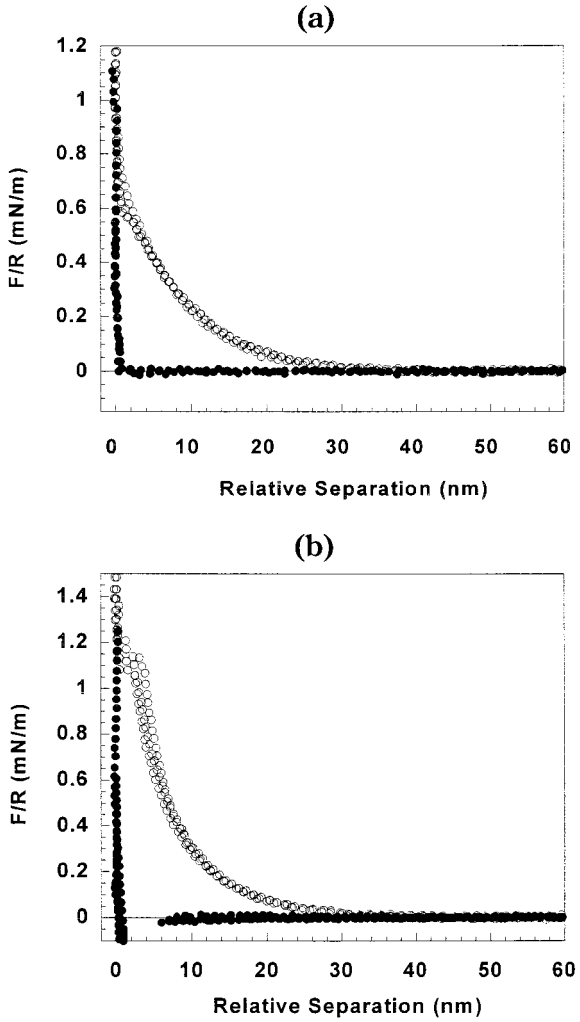

Figure 5. Colloid probe force measurements between silica colloids and plasma polymer surfaces in different PBS dilutions (pH 7.4). (a) Silica−Happ interactions: ○, 1:100 PBS; ●, 1:1 PBS. (b) Silica−Aapp interactions: ○, 1:100 PBS; ●, 1:1 PBS.

interacting with pure alkane interfaces, $3-7 \times 10^{-21}$ J.[61] Another possible explanation for the lack of an observed attraction is that the van der Waals forces are not resolved due to either nanometer scale surface roughness or plasma polymer chain extension into solution (generating a steric repulsive layer), both of which would effectively mask attractive forces if present. In the silica−acetaldehyde plasma polymer interaction (Figure 5b), a jump into contact was observed at both electrolyte concentrations, suggesting that van der Waals interactions were resolvable in this case. This indicates that both surface roughness and extension into solution of putative chain ends are minimal for the acetaldehyde plasma polymer, for the reasons discussed above. This is more consistent with AFM imaging measurements performed on both plasma polymer surfaces which have yielded root mean square roughnesses of <0.5 nm over several square micrometers both in air and aqueous environments.[40]

The marked effect on the surface forces of the addition of a layer of grafted poly(ethyleneimine) atop the acetaldehyde plasma polymer is shown in Figure 6. In both dilute and concentrated electrolyte concentrations, the force versus separation data showed a purely attractive relationship, which caused the surfaces to jump together at

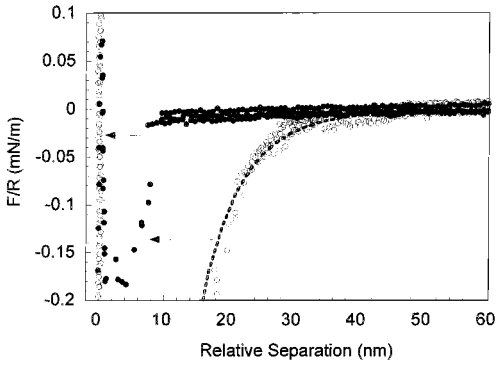

Figure 6. Colloid probe force measurements between silica colloids and PEI-modified Aapp surfaces in different PBS dilutions (pH 7.4). Arrows indicate inward jumps in data. ○, 1:100 PBS (DLVO fit to data: $\psi_{o1} = -50$ mV, $\psi_{o2} = +30$ mV, $1/\kappa = 6.6$ nm); ●, 1:1 PBS.

finite separations. Following this jump, a hard wall repulsion with minimal compressibility indicated a lack of significant steric interactions due to the polyelectrolyte grafted layer. On retraction of the silica colloid probe from the surface, significant adhesion was observed in all cases.

Both the range of the attractive force on the approach curve and the jump into contact occur at larger separations in the more dilute electrolyte system. The decay length of the long-range attractive force is found to be 6.8 nm in the dilute electrolyte system which is again in good agreement with the theoretical Debye length (6.6 nm). The fact that the attractive force collapses in range markedly at the increased electrolyte concentration also supports the electrostatic explanation for the attractive forces in dilute electrolyte solution. The fitting parameters used to generate the theoretical electrical double layer interaction profile shown in Figure 6 also agree perfectly with the ζ potential values obtained for both the PEI-grafted surface (+30 mV, see Figure 4b) and the silica colloid probe (ca. −50 mV[38]) under similar electrolyte conditions. This correlation has been observed previously for polyelectrolyte layers adsorbed on oppositely charged surfaces in dilute electrolyte solutions.[62] The behavior of the grafted PEI layer is thus entirely consistent with many previous experimental and theoretical studies of polyelectrolyte adsorption on oppositely charged surfaces, which frequently show flat conformations and charge reversal of the underlying substrate.[63]

The lack of polyelectrolyte extension into solution shown by the surface force measurements plus the XPS data both suggest a minimal quantity of polyelectrolyte on the surface. However, the charge reversal of the underlying acetaldehyde plasma polymer surface demonstrated by both the surface force and streaming potential measurements shows that there is still a large quantity of cationic (presumably amine) moieties at the interface free for subsequent reaction with polysaccharide. Thus, the use of the PEI interlayer as a support for subsequent polysaccharide grafting would appear to be justified.

AFM Colloid Probe Force Measurements on Polysaccharides Directly Grafted on Plasma Polymer Surfaces. Figure 7a shows the measured interaction forces between a silica colloid probe and the *n*-heptylamine plasma polymer surface bearing grafted high carboxyl density polysaccharide CMD 1:2 in different electrolyte concentrations. An exponential repulsion between the

(61) Mulvaney, P.; Perera, J. M.; Grieser, F.; Stevens, G. W. *J. Colloid Interface Sci.* **1996**, *183*.

(62) Hartley, P. G.; Scales, P. J. *Langmuir* **1998**, *24*, 6948−6955.

(63) Fleer, G. J.; Cohen Stuart, M. A.; Scheutjens, J. M. H. M.; Cosgrove, T.; Vincent, B. *Polymers at Interfaces*, 1st ed.; Chapman & Hall: London, 1993.

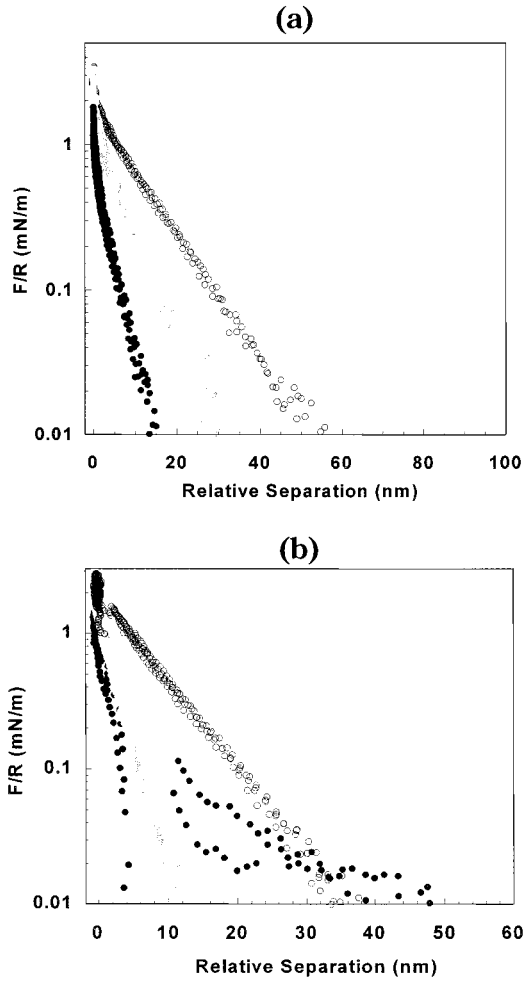

Figure 7. Colloid probe force measurements between silica colloids and polysaccharide-modified Happ surfaces in different PBS dilutions (pH 7.4). The data have been plotted on a log scale to highlight decay length variations. (a) Silica −HA−CMD 1:2: (open circles) 1:100 PBS, (gray circles) 1:10 PBS, (black circles) 1:1 PBS. (b) Silica−HA−CMD 1:30: (open circles) 1:100 PBS, (gray circles) 1:10 PBS, (black circles) 1:1 PBS.

colloid probe and the polymer surface was observed in all electrolyte conditions. A smooth transition was found between the exponential behavior and hard wall repulsion (designated as zero separation) without discontinuities characteristic of attractive force jumps. No adhesion was observed on retraction of the probe from the surface. The exponential repulsions exhibited a marked electrolyte dependence, reducing in range as the electrolyte concentration was increased. While this behavior appears analogous to the electrical double layer compression observed for the unmodified plasma polymer surfaces, comparison of the measured versus theoretical decay lengths for the electrolyte systems (Table 2) reveals considerable discrepancies. This is particularly true at the higher electrolyte concentrations, where the range of the measured interactions greatly exceeds that predicted for a purely electrostatic interaction.

These data strongly suggest the presence of a compressible layer resulting from the grafting of the polysaccharide on the plasma polymer surface, with confinement of this layer during approach of the silica colloid probe resulting in a steric repulsion between the surfaces.

The onset of this repulsive interaction at separations of 15−50 nm would be expected to correspond approximately to the polysaccharide extension from the plasma polymer surface in the different electrolyte concentrations. These values are considerably larger than the nominal polymer layer thicknesses extracted from the XPS data presented in Figure 2, where the presence of a significant C−C component from the underlying plasma polymer suggests that the polysaccharide layers are restricted to within 10 nm of the plasma polymer surface. This discrepancy presumably results from rearrangement of the interface during dehydration/evacuation prior to XPS analysis.

The origin of the electrolyte concentration dependence in the range of these steric interactions likely lies with the conformation of the polysaccharide at the interface. The streaming potential data in Figure 4a demonstrate that both the polysaccharide and the underlying plasma polymer carry a substantial negative charge at the pH of these experiments (pH 7.4). Under these conditions, intrapolysaccharide (i.e., segment−segment) and polysaccharide−substrate interactions are electrostatically repulsive and poorly screened due to the low electrolyte concentration. The polysaccharide would, thus, be expected to be repelled electrostatically from the surface, stretching the polysaccharide chains and resulting in a lower concentration close to the surface. This extended conformation would then result in a maximum range of interaction with an impinging colloid probe (or other macromolecular species).[63]

By addition of background electrolyte, both the segment−segment and segment−plasma polymer repulsions are increasingly screened. This allows the polymer to adopt a more random coil configuration and thus to move its center of mass closer to the plasma polymer surface, resulting in a less extended graft layer structure. The effect of this behavior on the surface forces is that the impinging silica colloid particle senses the polysaccharide at smaller separations between it and the underlying plasma polymer surface; that is, the range of the steric repulsion between the surfaces is reduced in this "salted brush" regime.[63] Other research has further suggested that at low electrolyte concentration, in the so-called "osmotic brush" regime, grafted weak polyelectrolyte layers in fact adopt a less extended conformation, due to a reduction in their degree of dissociation as they struggle to maintain electroneutrality. This results in a maximum in the extension at intermediate electrolyte concentrations (typically $\sim 10^{-2}$ M).[63,64] No such maximum in the extension of CMD 1:2 was observed in the electrolyte concentration range studied, due to either the high "strength" of the carboxyl groups or branching within the polysaccharide chains.

Figure 7b shows the results of AFM force measurements between a silica colloid probe and a *n*-heptylamine plasma polymer surface bearing grafted low density carboxymethylated dextran (CMD 1:30). At lower electrolyte concentrations (1:100 and 1:10 PBS), the data appear qualitatively similar to the measurements made between a silica colloid probe and a bare plasma polymer surface. These consist of exponential repulsions whose decay lengths compare favorably with that expected for a purely electrostatic repulsion in similar electrolyte conditions (see Table 2). At the lowest electrolyte concentration, a jump is observed in the data at the transition between exponential repulsion and hard wall contact which is indicative of attractive van der Waals forces operating between the surfaces. In addition, adhesion was observed on retraction of the probe from the surface in most cases.

(64) Wesley, R. D.; Cosgrove, T.; Thompson, L.; Armes, S. P.; Billingham, N. C.; Baines, F. L. *Langmuir* **2000**, *16*, 4467−4469.

This suggests minimal extension of the CMD 1:30 polysaccharide from the surface which would otherwise tend to obscure these behaviors. Only at the highest electrolyte concentration (1:1 PBS) is there evidence of short-range steric interactions (~5 nm in extent), as evidenced by deviations from the purely electrostatic decay length. In addition, at this electrolyte concentration we observe erratic longer range repulsive forces. This behavior may represent the extension of sparse polymer chains from the surface in these conditions or be due to adhesion and extraction of polysaccharide chains during the repeated impact of the colloid probe on the grafted layer.

All of the above behaviors, as well as the XPS overlayer calculations discussed earlier, indicate a low concentration of polysaccharide at the interface. This is presumably due to the low carboxyl density of this polysaccharide resulting in a lower pinning density, as has been discussed previously.[15] This also provides further support for the hypothesis that the ζ potential behavior observed for the heptylamine plasma polymer−CMD 1:30 surface in Figure 4a contains within it a substantial contribution from the underlying plasma polymer, since it appears intermediate between the behaviors of the bare heptylamine plasma polymer and high carboxyl density carboxymethyldextran−heptylamine plasma polymer coatings.

AFM Colloid Probe Force Measurements on Polysaccharides Grafted via Polyelectrolyte Interlayers. The surface forces experienced on approach of the silica colloid probe to the acetaldehyde plasma polymer−PEI support surface following the attachment of the high carboxyl density polysaccharide CMD 1:2 are shown in Figure 8a. The data show an electrolyte-dependent long-range exponentially repulsive force and a smooth transition to the hard wall repulsion designated as zero separation. No attractive component was detected in any of the force curves, indicating removal or masking of both the van der Waals and electrostatic attractive forces observed in Figures 5b and 6, respectively. No adhesion was experienced between the colloid probe and the surface following retraction. The removal of the electrostatic attraction is explained by recourse to the streaming potential data (Figure 4b) which show that attachment of the CMD 1:2 to the PEI−Aapp interlayer results in charge reversal of the surface, yielding a ζ potential of −60 mV at pH 7.4 in dilute electrolyte. Comparison of the decay length of the exponential portions of the data with the theoretical Debye length (Table 2) yields no agreement under any of the electrolyte conditions, suggesting a nonelectrostatic origin to the repulsive forces.

Once again, these data strongly suggest the presence of a compressible hydrated layer resulting from the grafting of the polysaccharide on the plasma polymer/PEI surface. Confinement of this layer during approach of the silica colloid probe generates a steric repulsion between the surfaces. This is perhaps counterintuitive, given the nature of the underlying PEI−plasma polymer interface. One might assume, given the nature of the PEI−Aapp surface, that it might behave as a flat oppositely charged surface for the attachment of the polysaccharide. Under these conditions, the polysaccharide would be expected to adsorb, and presumably graft, in a flat conformation on the surface, as per the PEI grafting on the underlying acetaldehyde plasma polymer. This is akin to the "side-on" attachment suggested previously.[6,17] The fact that such a flat conformation was not observed suggests that the PEI underlayer does not, in fact, behave as a flat grafting surface. Bearing in mind that the CMD 1:2 grafting reaction relies on the consumption and conversion of amine groups into amides, it seems reasonable to suggest that the grafting reaction results in the neutralization of the PEI interlayer. The effect of such neutralization would be to reduce the affinity of the PEI layer for the underlying (anionic) plasma polymer. This, therefore, provides a mechanism for both removal of cationic surface charge and extension of the PEI−CMD 1:2 interlayer from the surface. Such extension would also likely result in the exposure of fresh reaction sites for the CMD 1:2 to attach to the PEI, resulting in an enhanced "three-dimensional" graft support. The result of this process would be the production of an outer extended anionic CMD 1:2 surface, a partially or completely neutralized/amphoteric PEI−CMD 1:2 complex interlayer, and a neutral or anionic acetaldehyde plasma polymer surface as the substrate. Such an explanation would also support the apparent distribution of PEI nitrogen-containing species throughout the CMD 1:2 layer, observed in the XPS measurements discussed earlier.

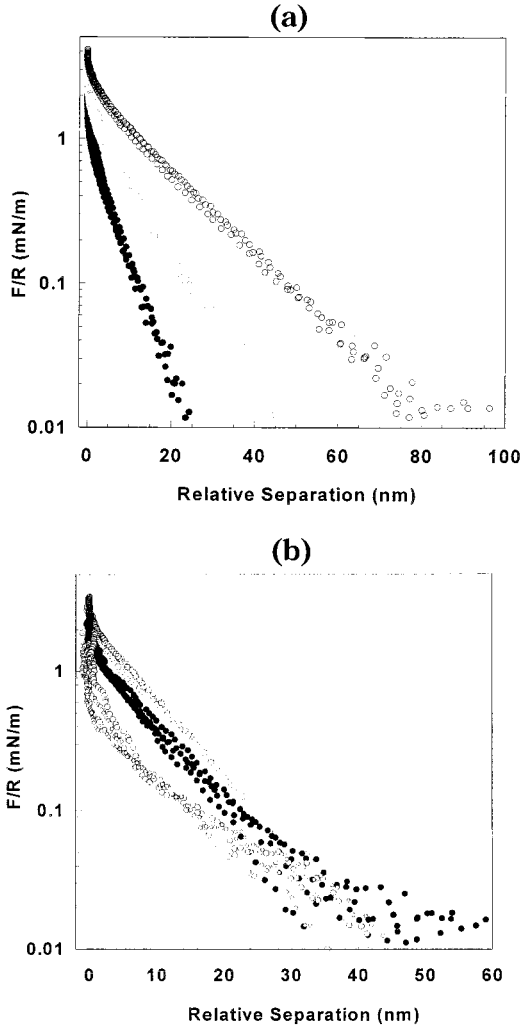

Figure 8. Colloid probe force measurements between silica colloids and polysaccharide-modified Aapp surfaces in different PBS dilutions (pH 7.4). The data have been plotted on a log scale to highlight decay length variations. (a) Silica−Aapp−PEI−CMD 1:2: (open circles) 1:100 PBS, (gray circles) 1:10 PBS, (black circles) 1:1 PBS. (b) Silica−Aapp−PEI−CMD 1:30: (open circles) 1:100 PBS, (gray circles) 1:10 PBS, (black circles) 1:1 PBS.

Under these circumstances, the extension of the outer CMD 1:2 polysaccharide coating would be controlled largely by its intralayer electrostatic interactions, as discussed earlier. The extended conformation resulting from these interactions leads to a long-range interaction with

impinging species and hence, in this study, a maximum in the range of the repulsive forces experienced by the silica colloid probe approaching the polysaccharide surface. By addition of background electrolyte, the segment−segment repulsions are screened allowing the polysaccharide to move its center of mass closer to the plasma polymer surface. The result is that the impinging silica colloid particle first senses the polysaccharide when it is closer to the plasma polymer surface; that is, the range of the steric repulsion between the surfaces is reduced. This behavior would explain the sequential reduction in the range of the repulsive surface forces measured in this study between the silica colloid probe and CMD 1:2 surface as electrolyte was added to the system.

We note that the maximum range of the repulsive forces for the CMD 1:2 surface grafted using the PEI interlayer is some 1.6−1.8 times greater in all electrolyte concentrations than that found by grafting the same polysaccharide directly onto the heptylamine plasma polymer (see Figure 7b). This may suggest either a higher graft density, resulting in a more extended polysaccharide conformation, or a thicker layer due to the presence of the PEI interlayer.

Either mechanism would be consistent with a three-dimensional interlayer providing either additional extension or simply an increased polysaccharide grafting efficiency. The latter assertion, however, is supported by the XPS measurements on both of these surfaces, which showed an increase in the O/C ratio, from 0.3 to 0.44 when the amine-rich interlayer was employed (see Table 1). This indicates an increased polysaccharide surface concentration when the interlayer is used.

Surface force measurements recorded during approach between a silica colloid probe and the Aapp−PEI surface bearing a secondary grafted layer of low carboxyl density carboxymethyldextran (CMD 1:30) are shown in Figure 8b. Once again, the force versus separation relationship is repulsive at all electrolyte concentrations. Interestingly, the electrolyte dependence of the repulsion noticed in the previous examples is removed, with the data showing a maximum range of ∼40 nm in all electrolyte concentrations. Thus, it appears that this coating presents a steric barrier whose hydrated extension is not governed by electrostatic interactions within the layer.

The data recorded on these surfaces were also considerably "noisier" than those for any of the other surfaces measured; that is, the force curves did not follow the smooth exponential repulsions characteristic of the other measurements. In addition, frequent adhesions were observed between the colloid probe and surface and in some cases weak, irreproducible minima in the data at separations in excess of 45 nm. The lack of significant electrolyte dependence in the steric interactions is perhaps not surprising when we consider the streaming potential data (Figure 4b), which show that this surface is only weakly charged in the dilute electrolyte solution at pH 7.4 (ζ potential < -20 mV). As suggested earlier, this likely results from the low level of charge and lower pinning density of the polysaccharide in this case as well as the consumption of carboxylate groups during the grafting reaction. In addition, neutralization of surface charge via simple charge−charge complexation between the cationic PEI and the anionic carboxyl groups on the polysaccharide would be expected to consume a greater proportion of the lower number of carboxyls present on this polysaccharide relative to the PEI−CMD 1:2 surface. This would result in a more amphoteric graft layer structure, potentially carrying both free carboxyl and free amine functionalities within it. These mechanisms would be expected to lead to a minimization of intralayer repulsive electrostatic interactions. If this were the case, then the importance of electrolyte screening of such interactions in determining the conformation of the graft layer, and thus the range of the steric repulsive forces, would be expected to be reduced. This would in turn explain the lack of electrolyte dependence in the measured repulsive forces.

It is not immediately clear why the force versus distance curves recorded against this surface were more variable in nature. We tentatively suggest that this may indicate the presence of domains of restricted polymer mobility within the coating, which result from both the grafting reaction and putative polysaccharide−PEI charge complexes. Relaxation of such regions following compression beneath the colloid probe would be expected to be slow, and thus successive approach−retract cycles would be expected to show variation. In addition, localized cationic functionality within the coating, which may not have been consumed during grafting due to the low carboxyl density of the polysaccharide, would readily attach (i.e., bridge) to the anionic silica colloid probe. This might further explain the long-range attractive minima observed on several occasions as well as the adhesive forces observed during retract cycles. The dependence on the surface forces of approach−retract velocity would provide further evidence for such processes; however, these data are not available in the current study.

Conclusions

A variety of surface analysis techniques have been employed in order to characterize surfaces bearing grafted carboxylated polysaccharides as well as the support layers to which they were attached. The data demonstrate that a densely carboxylated polysaccharide (CMD 1:2) exhibited an extended layer conformation on the surfaces in aqueous solution, either when grafted directly on a flat amine plasma polymer surface or via an amine-rich polyelectrolyte interlayer. This was likely the result of increased efficiency of the grafting reaction, which relies on the reaction of polysaccharide carboxyl groups with surface amines.

Streaming potential and XPS data also showed that a significant excess of carboxyl functionality on these grafted surfaces imparted a strong negative charge at neutral pH, even when the amine-rich PEI interlayer, itself strongly cationic, was employed as a graft support.

For the lower density polysaccharide, the amine-rich interlayer was required to increase the polysaccharide surface concentration to an appreciable level, as ascertained from XPS measurement. AFM colloid probe measurements similarly showed that the interlayer was required to introduce steric repulsions between the probe and the surface, a further indication that a higher graft density was achieved using this method.

The interaction between the anionic silica colloid probe and the densely carboxylated polysaccharide surfaces showed "electrosteric" interactions resulting from the repulsion between the probe and the polysaccharide layer due to both charge−charge and steric interactions resulting from the confinement of the polysaccharide between the probe and underlying surface. The electrolyte dependence of these interactions indicated that intralayer charge−charge interactions were also important in establishing the polysaccharide conformation at the interface. No such dependence was observed for the low carboxyl density polysaccharide grafted via the polyelectrolyte interlayer. This, in combination with a low ζ potential over a broad pH range (as derived from streaming potential measurements), suggests that the polysaccharide con-

formation was less reliant on intralayer charge interactions in this case. These measurements in conjunction with XPS suggest that the chemistry of the layer contains contributions from both the polysaccharide and polyelectrolyte interlayer. This indicates that during the grafting reaction, the polyelectrolyte (which is initially strongly associated with the underlying plasma polymer substrate) dissociates somewhat and becomes intercalated within the polysaccharide layer, resulting in an amphoteric layer composed of both polyelectrolyte and polysaccharide moieties.

Thus, the mode of grafting in conjunction with intralayer electrostatic interactions determine the three-dimensional structure of the grafted polysaccharide layers, their extension into solution, and therefore their effectiveness as steric barrier layers. For all grafted polysaccharide surfaces, the range of the steric repulsive forces in aqueous electrolyte exceeded the nominal layer thicknesses derived from XPS data. This highlights the dangers inherent in using XPS data as an indicator of polymer extension in aqueous environments and contradicts earlier suggestions that steric forces are a minor contributor to the interactions between polysaccharide surfaces and impinging species.[11,30] These observations have important implications for the understanding of the protein and cell repellency properties of these physicochemically distinct polysaccharide surfaces, which will be discussed in forthcoming publications.[36,37]

Acknowledgment. Peter Scales (Chemical Engineering Department, University of Melbourne) is gratefully acknowledged for useful discussions and for providing access to the streaming potential apparatus used in this study. Thomas Gengenbach (CSIRO Molecular Science) provided valuable guidance concerning interpretation of XPS data. S.L.M. acknowledges support from a postgraduate scholarship from the ARC cooperative research center for Eye Research and technology.

LA001801I